

Thus, the sufficient conditions for the formation of a moving pole for  $\gamma_1^{i+1} < 0$  are the following (at  $\xi = 0$ ): a) all  $g_{1,2}^{ik} < 0$  ( $i \neq k$ ) or b) all  $g^{i+k} \ll (g/n!)(g_1^{i+1}/g)^n$ . This means that on the right sides of Eq. (9) we have left only terms with  $\gamma_1^{i+1}$  from (5) and at some  $\xi$ , all the  $\gamma_k^{ik}$  become less than zero.

If  $\gamma_1^{i+1} > 0$ , then the moving pole is formed under the conditions: c)  $g_1^{i+2} < 0$ ,  $g_1^{i+3} > 0$ , ... all  $g_2^{ik} < 0$  or b). Here all the  $\gamma_1^{ik}$  will have alternating signs. Therefore the singularity appears at  $q \neq 0$ . For example, for a square lattice of chains,  $\mathbf{q} = [\pi, \pi]$ .

<sup>1</sup>We shall also make use of the mixed representation. The momentum along the corresponding chain and its number are indicated here. On each chain, the electrons occupy in the one-dimensional reciprocal cell the region between  $-\rho_F$  and  $+\rho_F$ . We then make use of the term "Fermi point."

<sup>2</sup>In place of  $g^{ik}$ ,  $\gamma^{ik}$ , we shall also use the notation  $g^{i+n}$ ,  $\gamma^{i+n}$ , where  $n$  is the minimum number of transitions between near-

est chains, which must be undergone in order to proceed from chain  $i$  to chain  $k$ . For the quantities  $g^{it}$ ,  $\gamma^{it}$ , we shall use the notation  $g$ ,  $\gamma$ .

<sup>3</sup>The Fermi momenta are the same in both subsystems. The difference in the Fermi energies can be removed by renormalization of the constants. But the variables  $\xi^{a,b} = \ln(\bar{\omega} / \max\{T, \omega, v_F^{a,b} p\})$  are nevertheless all differently defined because of the difference between the Fermi velocities. Therefore, Eqs. (9) can be written down only at  $\omega = 0$ ,  $p = 0$  in the investigation of the temperature dependence of  $\gamma(\xi)$ .

<sup>1</sup>I. E. Dzyaloshinskiĭ and A. I. Larkin, Zh. Eksp. Teor. Fiz. 61, 791 (1971) [Sov. Phys. JETP 34, 422 (1972)].

<sup>2</sup>L. P. Gor'kov and I. E. Dzyaloshinskiĭ, Zh. Eksp. Teor. Fiz. 67, 397 (1974) [Sov. Phys. JETP 40, 198 (1974)].

<sup>3</sup>L. N. Bulaevskiĭ, Usp. Fiz. Nauk 115, 263 (1975) [Sov. Phys. Uspekhi 18, 131 (1975)].

<sup>4</sup>A. Z. Patashinskiĭ and V. L. Pokrovskiĭ, Fluktuatsionnaya teoriya fazovykh perekhodov (Fluctuation Theory of Phase Transitions) Nauka, 1975, Sec. 3.

Translated by R. T. Beyer

## Energy spectrum of the donors in GaAs and Ge and its reaction to a magnetic field

E. M. Gershenson, G. N. Gol'tsman, and A. I. Elant'ev

Moscow State Pedagogical Institute

(Submitted July 1, 1976)

Zh. Eksp. Teor. Fiz. 72, 1062-1080 (March 1977)

The spectrum of the submillimeter photoconductivity of  $n$ -GaAs and  $n$ -Ge in a magnetic field up to 60 kOe at helium temperatures was investigated. A large number of lines due to transitions between excited states of the donors have been investigated, and the measurement results were used to determine a number of levels of the energy spectrum in a wide range of magnetic fields. For GaAs, these data are compared with calculations of the energy spectrum of the hydrogen atom in magnetic fields up to  $\sim 2 \times 10^9$  Oe. For the donors in Ge, the energy spectrum is investigated at different orientations of the magnetic field relative to the crystallographic axes ( $\mathbf{H} \parallel [100], [111], [110]$ ), and these results are also compared with the corresponding calculations.

PACS numbers: 72.40.+w, 72.60.+g

### INTRODUCTION

The photoexcitation spectrum of shallow impurities in many superconductors lies in the submillimeter band and makes it possible to obtain information not only on the properties of the impurities, and particularly on its energy spectrum, but also on the semiconducting crystal itself. The results of submillimeter spectroscopy of semiconductors are of interest for atomic spectroscopy. By using as a model a shallow impurity in a semiconductor, it is possible to obtain in a number of cases experimental data which cannot be obtained by studying the atoms in free space. A sufficiently well-known example is the problem of the properties of atoms in very strong magnetic fields. Indeed, from the point of view of the influence on the impurity-atom spectrum, the effective magnetic field is equivalent to one that is larger by 4-6 orders of magnitude than in the case of atoms

in free space. This is caused by the small characteristic energies and by the strong interaction of the shallow-impurity atoms with the external magnetic field, a fact explained by the low effective mass  $m^*$  of the electron (hole) and the large dielectric constant  $\kappa$  of the medium—the semiconducting crystal. The impurity-atom spectrum therefore turns out to be strongly shifted towards longer wavelengths.

We have investigated the energy spectrum of shallow impurities in Ge and GaAs and the effect exerted on it by a magnetic field  $H$ , using for this purpose a highly sensitive backward-wave-tube (BWT) submillimeter spectrometer of high resolution.<sup>[1]</sup> It is customary to use for such measurements long-wave infrared gratings and interference spectrometers. In particular, three groups have recently published papers<sup>[2,3]</sup> on the spectroscopy of residual shallow impurities in ultrapure Ge

using modern Fourier spectrometers. However, interference instruments are still infrequently used for investigations in a magnetic field, and the spectral resolution is low: up to now (see, e.g., [4,5]) the Zeeman components could be resolved at  $H$  larger than several kOe, despite the fact that the orientation of the magnetic field was chosen such that the number of components is small, and their energy shift with increasing  $H$  was relatively large. The insufficient spectral resolution also impedes the study of the interaction of the Zeeman sublevels in magnetic-field orientations such that the field mixes the excited impurity stage with different values of the magnetic quantum number  $m$ .

The relatively low sensitivity of infrared instruments makes it possible to measure the photoexcitation spectra of only the ground state of shallow impurities. The quantitative study of the Zeeman spectrum is confined in this case to several levels, to which intense transition from the ground state are realized. In addition, the positions of the lines in the spectrum are influenced by an additional effect, which is not always easy to distinguish from the sought effect, namely, the field-dependent splitting and shift of the ground-state level, which depend strongly on the chemical nature of the impurity. Submillimeter lasers, which are highly monochromatic and have a sufficient power level to ensure high resolution and sensitivity, can substantially add to the possibility of investigating the impurity (see, e.g., [6,7]), but they are as yet not continuously tunable, and this limits the spectral investigations considerably.

The foregoing difficulties not only make for a poor experiment, but also preclude in a number of cases the possibility of a sufficiently reliable comparison of the obtained data with the existing theory. At the same time, the theory of the energy spectrum of a shallow impurity in a magnetic field has made considerable progress. This pertains primarily to the calculation of the spectrum of a hydrogen-like impurity in a semiconductor with an isotropic nondegenerate free band (for example, donors in GaAs). If we choose  $Ry^* = m^*e^4/2\hbar^2\kappa^2$  as the energy unit and  $r_0 = (\hbar c/2eH)^{1/2}$  as the length unit, then the Hamiltonian of such an impurity center, in the effective-mass approximation, can be written in a cylindrical coordinate system  $(\rho, \varphi, z)$ , with the  $z$  axis directed along the magnetic field, [8] in the same form as for the hydrogen atom:

$$\mathcal{H}_{is} = - \left( \frac{\partial^2}{\partial \rho^2} + \frac{1}{\rho} \frac{\partial}{\partial \rho} + \frac{1}{\rho^2} \frac{\partial^2}{\partial \varphi^2} + \frac{\partial^2}{\partial z^2} \right) + \frac{1}{2i} \frac{\partial}{\partial \varphi} + \frac{\rho^2}{16} - \frac{1}{(\rho^2 + z^2)^{1/2}} \left( \frac{2}{\gamma} \right)^{1/2}, \quad (1)$$

where  $\gamma = \hbar\omega_c/2Ry^*$  and  $\omega_c = eH/m^*c$  is the cyclotron frequency.

Until recently, the energy spectrum of a hydrogen-like atom was determined only in the case of a weak ( $\gamma \ll 1$ ) or a strong ( $\gamma \gg 1$ ) field. In recent papers, [7-10] the eigenvalues of (1) were obtained by a variational method in a wide range of magnetic fields ( $\gamma = 0 - 1.0$ ). The dependence on  $\gamma$  was determined for the energies of those states which correspond at  $\gamma = 0$  to hydrogen-like states with principal quantum numbers  $n = 1, 2, 3$ .

Despite the different choice of trial functions, the results of these calculations agree in many respects, although for a number of levels (such as  $3s$  and  $3d_0$ ) the dependence of the energy on  $\gamma$  turns out to be different in papers by different authors.

A more complicated case is that of a semiconductor with an anisotropic conduction band. In this case one calculates the eigenvalues of the Hamiltonian [11]

$$\mathcal{H}_{an} = \frac{1}{2m_{\perp}} \left[ \left( \hat{p}_x + \frac{e}{c} A_x \right)^2 + \left( \hat{p}_y + \frac{e}{c} A_y \right)^2 \right] + \frac{1}{2m_{\parallel}} \left( \hat{p}_z + \frac{e}{c} A_z \right)^2 - \frac{e^2}{\kappa r}, \quad (2)$$

where  $m_{\perp}$  and  $m_{\parallel}$  are the transverse and longitudinal effective masses, and  $A_x, A_y, A_z$  are the components of the vector potential. In analogy with the hydrogen-like case, a parameter  $\gamma = \hbar\omega_c/2Ry^*$  is introduced, where  $Ry^* = m_{\perp}e^4/2\hbar^2\kappa^2$  and  $\omega_c = eH/m_{\perp}c$ . Thus, the energy spectrum of shallow donors in Ge was determined in [12] by a variational method in the region of intermediate fields (up to  $\gamma = 0.7$ ). The levels  $1s, 2p_0, 2p_{\pm 1}, 3p_{\pm 1}$  were calculated at  $\mathbf{H} \parallel [111]$ . In [11,13], for two magnetic-field orientations ( $\mathbf{H} \parallel [111]$  and  $\mathbf{H} \parallel [100]$ ), they determined the dependence of the energy of the levels  $1s, 2p_0, 2s, 3p_0, 2p_{-1}$  on the magnetic field ( $0 \leq \gamma \leq 3$ ), but in these calculations, in contrast to the preceding ones, allowance was made for the influence of the magnetic-field component perpendicular to the symmetry axis of the constant-energy ellipsoid. It should be noted that one usually calculates only the lowest-lying states; for the higher excited states the calculations is more complicated. It is particularly difficult for acceptors.

The main purpose of the present study was to investigate experimentally the energy spectrum of shallow impurities; the present article is devoted to donors in GaAs and Ge, while the results of the investigations of acceptors will be given in a succeeding paper. [14] The choice of the semiconductor materials for the investigations was governed by several factors. First, GaAs and Ge are among the purest semiconductors, so that the spectral resolution can be relatively high and makes it possible to perform measurements with very weak fields  $H$  ( $\gamma = 0.005 - 0.002$ ). Second, the large values of  $\kappa$  and the small  $m^*$  make it possible to study the impurities, in the magnetic field  $H \approx 60$  kOe available to us, under conditions  $\gamma \approx 1$ . At the same time, another reason why it is attractive to start the experimental investigation of the impurity spectrum with donors in GaAs is that this spectrum is the simplest and has been theoretically well-investigated; furthermore, the short-wave limit of the spectrometer used by us does not prevent in this case observation of some of the lines of the photoexcitation of the ground state. The influence of the strong anisotropy of the effective mass on the energy spectrum manifests itself to full degree in the Zeeman spectrum of the donors in Ge. We have attempted to investigate the variation of the energy spectrum by applying a magnetic field not only along the directions that are customarily investigated both theoretically and experimentally, but also for the little-investigated case when the magnetic field is perpendicular to the symmetry axis of the constant-energy ellipsoid of the conduction band and there is no splitting of the levels with  $m = \pm 1$  in the weak-field approximation.

A study of independent interest is that of the interaction of the donor levels in Ge, when the magnetic-field component perpendicular to the symmetry axis of the constant-energy ellipsoid mixes the states of the donor electron and observation of anticrossing of levels becomes possible.

## EXPERIMENTAL PROCEDURE

The transitions of the electrons between the ground and excited states of the donors in GaAs and between the excited states of donors in GaAs and Ge were investigated with a BWT spectrometer<sup>[11]</sup> in the wavelength band  $\lambda = 3.5\text{--}0.25$  mm, corresponding to emission quantum energies 0.35–5 meV. The spectrometer resolution  $\Delta\varepsilon/\varepsilon$  reaches  $\approx 10^{-5}$ , but is actually determined by the width of the investigated lines, which amounts to  $\gtrsim 0.005$  meV. The absolute accuracy of the measurement of the radiation frequency, determined with the aid of an open resonator (of the Fabry-Perot type), is  $\approx 1$  GHz ( $\Delta\varepsilon \approx 0.003$  meV).

We investigated the photoconductivity spectra due to photothermal ionization<sup>[15]</sup> of the ground and excited states of donors in the magnetic field of a superconducting solenoid up to 60 kOe, and in the temperature interval 2–10 °K. The spectrum was scanned as a rule with a magnetic field, but if the line energy was weakly dependent on  $H$  or if the measurements were performed in the absence of  $H$ , then frequency scanning was used to record the spectrum.

We used  $n$ -Ge doped with Sb to a donor density  $N_d \approx 10^{12}\text{--}10^{13}$  cm<sup>-3</sup> and with P to a density  $\approx 10^{14}$  cm<sup>-3</sup>, with a compensation  $N_d/N_a \lesssim 20\%$ , as well as  $n$ -GaAs with  $N_d - N_a (0.5 - 2) \times 10^{14}$  cm<sup>-3</sup> and with an electron mobility  $(0.8 - 1.5) \times 10^5$  cm<sup>2</sup>/V-sec at  $T \approx 77$  °K.

The Ge samples were cut in the form of parallel-epipeds measuring  $4 \times 4 \times 2$  mm in the crystal planes (100), (111), (110), and were equipped with ohmic contacts. The plane of the sample was oriented perpendicular to the magnetic field and to the propagation direction of the submillimeter radiation. In a number of cases, the magnetic field was perpendicular to the direction of propagation of the radiation and parallel to one of the crystallographic axes: [100], [111], or [110] in the (110) plane parallel to the sample surface. The sample was oriented in the magnetic field with an adjusting device and the orientation was verified against the position of the cyclotron-resonance (CR) lines of the free electrons, registered in the photoconductivity spectrum in analogy with<sup>[16]</sup>. The orientation accuracy reached 2'.

The GaAs samples were made of epitaxial films with high-resistance substrate and had an area  $4 \times 4$  mm<sup>2</sup>. In a number of cases dimensions were much larger (20  $\times$  20 mm), to make the sample overlap the cross section of the submillimeter channel and maintain the direction of polarization of the radiation in the sample. Quite frequently, the polarization direction of the submillimeter radiation in the investigated Ge or GaAs sample could not be maintained strictly constant relative to the magnetic field, therefore one and the same spectrum

revealed simultaneously lines realized in accordance with the selection rule only at  $\mathbf{E}_\perp \parallel \mathbf{H}$  or only at  $\mathbf{E}_\perp \perp \mathbf{H}$ .

The free carrier density ( $n$ ) in the investigated sample consisted of the density of the nonequilibrium carriers ( $n_{eq}$ ) and of the equilibrium carriers ( $n_b$ ) generated by the background radiation at room temperature. The temperature dependence of the photoresponse ( $\Delta\sigma/\sigma$ ) due to the photothermal ionization of the excited states of the impurity can be approximately calculated at low temperature in the following manner:

$$\frac{\Delta\sigma}{\sigma} = \frac{\Delta n}{n} \sim \frac{n_{st}(T) w_f(T) \tau(T)}{n_{eq}(T) + n_b} \sim \exp\left(-\frac{\varepsilon_g - \varepsilon_{st}}{kT}\right) \exp\left(-\frac{\varepsilon_f}{kT}\right) \tau(T) \left[ \frac{N_d - N_a}{2N_a} N_c \exp\left(-\frac{\varepsilon_g}{kT}\right) + n_b \right]^{-1}, \quad (3)$$

where  $n_{st}$  is the carrier density at the starting level of the transition,  $w_f$  is the probability of thermal ionization of the final state of the transition,  $\varepsilon_g$ ,  $\varepsilon_{st}$ , and  $\varepsilon_f$  are the respective ionization energies of the ground level of the impurity, of the starting level of the transition, and of the final level of the transition, while  $\tau$  is the free-carrier lifetime. It follows from (3) that the photoresponse is maximal at a temperature such that the contribution of the equilibrium free electrons to the sample conductivity  $\sigma$  exceeds somewhat the contribution of the nonequilibrium electrons. In our experiments, the intensity of the background radiation was such that the maximum of the photoresponse for Ge corresponded to  $T \sim 6\text{--}8$  K. The electric field  $E$  in the Ge sample was usually chosen of the order of 0.3–1 V/cm. This value of  $E$  is still too low to lead to the observed changes in the energy spectrum of the impurities, and in such a field there is still no impact ionization of the impurities by the free carriers, when the low-frequency noise at the contacts of the investigated sample increases sharply.

Measurements of  $n$ -GaAs were sometimes carried out with weak additional interband excitation of the sample by an incandescent lamp (just as in the preceding study<sup>[17]</sup>), since this led to a narrowing of the spectrum line as a result of impurity charge exchange; the value of  $E$  in the sample was chosen somewhat lower than the impurity impact-ionization field.

At  $\mathbf{H} \parallel [111]$  there are in Ge two groups of nonequilibrium equal-energy ellipsoids of the conduction band: for one ellipsoid, the magnetic field is parallel to the symmetry axis (we designate this case A, just as in<sup>[11]</sup>), and for the three others at an acute angle to this axis (case B). In the  $\mathbf{H} \parallel [100]$  orientation, all four ellipsoids are equivalent (case C). In the  $\mathbf{H} \parallel [110]$  orientation, the magnetic field for two ellipsoids is directed perpendicular to the symmetry axis (E), and for the remaining two at an acute angle to this axis (D). Zeeman line components belonging to nonequivalent valleys of the conduction band and appearing in one and the same spectrum (e.g.,  $2p_{0,A} - 2s_A$  from  $2p_{0,B} - 2s_B$ ) can be distinguished by their splitting following a small disorientation of the sample (in which case, e.g.,  $2p_{0,A} - 2s_A$  is not split but  $2p_{0,B} - 2s_B$  splits into three lines belonging to different valleys of the conduction band).

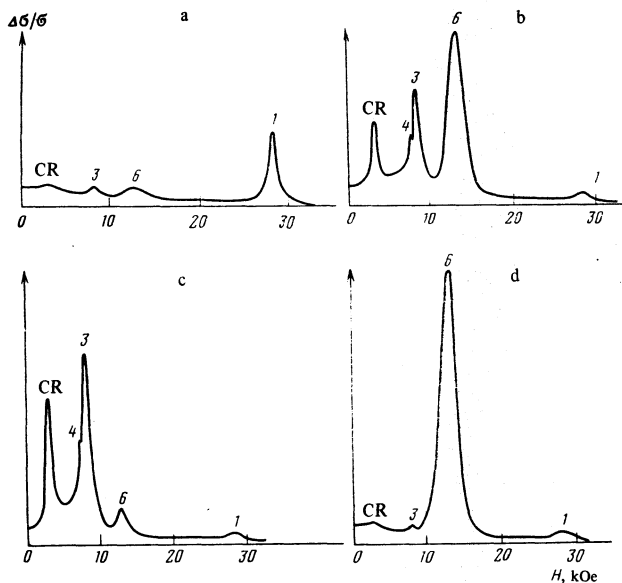


FIG. 1. Photoconductivity spectra of  $n$ -GaAs,  $\lambda = 1.58 \cdot 10^3 \mu$ ,  $T = 4.2^\circ \text{K}$ . The radiation propagates perpendicular to  $\mathbf{H}$ : a— $\mathbf{E} \parallel \mathbf{H}$ ; b— $\mathbf{E} \perp \mathbf{H}$ . The radiation propagates parallel to  $\mathbf{H}$ ; c—right-hand circular polarization; d—left-hand circular polarization. The numbers on the lines correspond to the numbers in Table I.

## EXPERIMENTAL RESULTS AND DISCUSSION

### Donors in GaAs

1. The photoconductivity spectrum of  $n$ -GaAs was investigated by us in a magnetic field up to 60 kOe and is compared with the recently published theoretical<sup>[8-10]</sup> and experimental studies.<sup>[7]</sup> Some of the data for a narrower range of emission-quantum energies  $\varepsilon$  and magnetic fields  $H$  was published earlier.<sup>[17]</sup>

At the same time, at the present state of the theory (e.g.,<sup>[18]</sup>) we can identify only five of the measured 14 transitions between the excited donor states, four of them being transitions between levels with  $n = 2$ .

Figure 1 shows the photoconductivity spectra of  $n$ -GaAs ( $T = 4.2 \text{ K}$ ), recorded with magnetic-field sweep at  $\lambda = 1.58 \cdot 10^3 \mu$  and at different radiation polarizations, namely,  $\mathbf{E}_\perp \parallel \mathbf{H}$  ( $\pi$  polarization) and  $\mathbf{E}_\perp \perp \mathbf{H}$ —the radiation propagates perpendicular to  $\mathbf{H}$  and parallel to  $\mathbf{H}$  (right and left circular polarizations,  $\sigma_+$  and  $\sigma_-$ , respectively). One can see the electron CR line and the photothermal-ionization lines of the excited states of the donors. Table I lists the corresponding experimental values of the energies of the spectral lines in the entire investigated range of  $\varepsilon$  and  $H$ . The line labels are the same as in the preceding paper.<sup>[17]</sup>

Figure 2 shows two photoconductivity spectra of  $n$ -GaAs ( $\lambda = 295 \mu$ , sweep of field  $H$ ,  $T = 4.2 \text{ K}$ ). The only transitions observed here are those from the  $1s$  ground state to the  $2p_{-1}$  excited state of the donors. The results of these measurements are also given in Table I.

2. Each transition from the ground state of the donors corresponds to several lines, a fact attributed by Fetterman *et al.*<sup>[19]</sup> to the presence in the sample, in

TABLE I. Energy (meV) of the photoconductivity-spectrum lines\* of shallow donors in GaAs in a magnetic field.

$H, \text{kOe}$	Number of line (polarization)													
	III ( $\sigma_-$ )	IV ( $\sigma_-$ )	V ( $\sigma_-$ )	VI ( $\sigma_-$ )	VII ( $\sigma_-$ )	VIII ( $\sigma_-$ )	3 ( $\sigma_+$ )	6 ( $\sigma_-$ )	10 ( $\pi$ )	12 ( $\sigma_+$ )	14	16 ( $\sigma_-$ )		
2.5	—	4.24	—	—	—	—	—	—	—	1.20	1.48	—	—	
6.0	—	4.11	—	4.07	—	4.03	—	0.7	—	1.76	2.90	—	—	
8.0	—	4.06	—	4.04	—	3.99	0.7	0.71	1.14	2.14	—	—	—	
10	—	4.04	—	4.00	—	3.96	0.89	0.76	1.22	2.47	—	—	—	
13	4.04	4.03	—	3.98	—	3.94	1.14	0.79	1.35	—	—	—	—	
20	4.04	4.03	—	3.99	—	3.95	1.64	0.86	1.64	—	—	—	0.38	
25	—	4.05	4.03	4.02	—	3.97	1.92	0.91	1.82	—	—	—	0.40	
30	—	4.09	4.07	4.06	4.03	4.01	2.13	0.95	1.98	—	—	—	0.42	
35	—	4.14	4.12	4.10	4.07	4.05	2.35	0.99	2.12	—	—	—	0.45	
40	—	4.19	4.17	4.15	4.11	4.09	2.55	1.02	2.26	—	—	—	0.48	
50	—	4.29	4.27	4.25	4.21	4.19	2.91	1.08	2.51	—	—	—	0.52	
55	—	—	—	—	—	—	3.01	1.11	2.64	—	—	—	0.54	

$H, \text{kOe}$	I ( $\sigma_-$ )	II ( $\sigma_-$ )	1 $\pi$	2 ( $\sigma_+$ )	4 ( $\sigma_+$ )	5 ( $\sigma_+$ )	7	8 ( $\pi$ )	9	11 ( $\sigma_+$ )	13	15
1.0	—	—	—	—	—	—	—	—	0.73	0.92	0.92	—
4.0	4.28	—	—	—	—	—	—	II P	1.34	1.39	—	—
6.0	4.19	—	—	—	0.50	—	—	—	0.75	1.66	1.84	—
8.0	4.15	—	—	—	0.67	—	—	—	0.86	2.01	2.29	—
10	4.12	—	—	0.61	0.86	—	—	0.72	0.95	2.34	2.71	—
13	4.10	—	—	0.73	1.14	1.65	—	—	1.10	2.86	3.37	—
16	4.09	—	—	0.88	1.45	1.89	—	—	0.88	1.21	3.38	—
20	4.11	—	0.626	1.00	1.92	—	—	—	1.01	1.34	—	—
25	4.15	4.13	0.71	1.16	—	—	—	—	1.16	1.50	—	0.66
35	4.24	4.22	0.87	1.50	—	—	—	—	1.09	1.40	1.79	—
40	4.30	—	—	1.66	—	—	—	—	1.19	1.52	—	0.74

\*The line designations correspond to<sup>[17]</sup> and to the figures.

comparable concentrations, of several chemically different shallow donors whose ground states differ little in energy. Up to four such components were observed in<sup>[19-21]</sup>; it is seen from Fig. 2 that their number can be also larger (up to 8). Experiments have shown that the ratio of the intensities of the components can vary substantially. An example of such a degradation is illustrated in Fig. 2; The spectrum of the  $n$ -GaAs changed in the course of time from *a* to *b*. The reason for this is unclear to us. The eight components can correspond to the impurities O, S, Se, and Te, which replace Ga, and C, Si, Ge, and Sn, which replace As. The ground-state energies of these impurities should, according to calculations,<sup>[22]</sup> coincide pairwise, but if they differ nevertheless, then the presence of all these impurities in one sample leads to the appearance in the spectrum of four pairs of close lines, as is indeed observed in our experiment. However, the fact that the ratio of the intensities is not constant seems strange from this point of view.

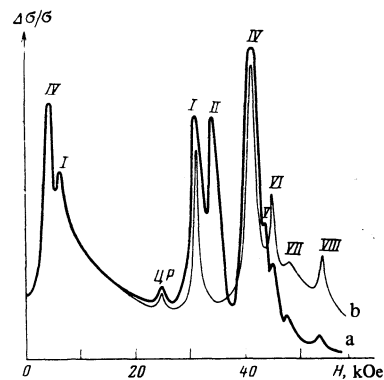


FIG. 2. Photoconductivity spectrum of  $n$ -GaAs at  $\lambda = 295 \mu$  and  $T = 4.2^\circ \text{K}$ . The numbers on the lines correspond to the numbers in Table I.

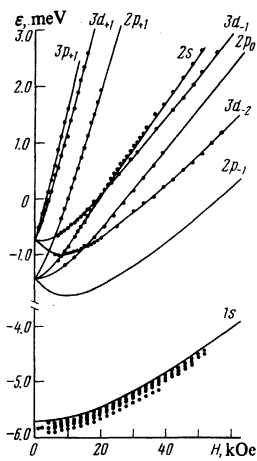


FIG. 3. Comparison of the theoretical and experimental energy spectra of shallow donors in GaAs in a magnetic field. Points—experiment; solid lines—theory.<sup>[7,8]</sup> The spectra are normalized to the  $2p_{-1}$  level.

A comparison of our results of the measurements of the  $1s - 2p_{-1}$  transition with the published data shows that the four components of the line  $2s - 2p_{-1}$  cited in seem to correspond to the components I, IV, VI, and VII, while the three components measured in<sup>[21]</sup> correspond to V, VI, and VIII, respectively. This comparison, however, is made difficult by the fact that the published data are not always presented in numerical form (more frequently in the form of graphs and spectra), and a reliable comparison calls in this case for at least a 0.2% accuracy in the determination of the line energy. Moreover, since the impurity concentrations in the samples used by us and by others<sup>[20,21]</sup> differ noticeably, even a very small line shift due to the interaction between impurities can lead to errors in the comparison of the data.

The multicomponent character of the transition lines and the associated experimental difficulties are practically nonexistent when the energy spectrum of the donors is investigated by measuring the spectrum of the transitions between the excited states.

3. To identify the spectral lines of the excited states of the donors in GaAs we compared the energy positions of the lines with calculation in a wide range of  $H$ , and used other data (for example, the relative line intensities, including data obtained at a different polarization of the radiation, see Fig. 1). It turned out that 9 of the 16 lines have an energy close to the calculated one. For these lines, the calculations by the different authors are close to one another. In the table, these are the lines 1 (transition  $2p_0 - 2s$ ), 2 ( $2p_{-1} - 2p_0$ ), 3 ( $2p_{-1} - 2s$ ), 4 ( $2s - 2p_{+1}$ ), 5 ( $2p_0 - 2p_{+1}$ ), 6 ( $2p_{-1} - 3d_{-2}$ ), 10 ( $2p_{-1} - 3d_{+1}$ ), 11 ( $2p_0 - 3d_{+1}$ ) and 12 ( $2s - 3p_{+1}$ ).

Let us compare the experimentally obtained energy spectrum of the donors in GaAs, in a wide  $H$  interval, with the theoretical one<sup>[7,8]</sup> (see Fig. 3). To this end, we use one level as a reference ( $2p_{-1}$ ). It is seen that the dependence of the energies of the levels  $2p_{±1}$ ,  $2p_0$ ,  $2s$ ,  $3p_{±1}$ ,  $3d_{±1}$ , and  $3d_{±2}$  on the magnetic field is described by the present calculations with accuracy not less than  $\approx 0.005 \text{ Ry}^*$ , which amounts to  $\approx 0.03 \text{ meV}$  for GaAs, but there is no such correspondence for the ground state.

The identification of the remaining transitions between the excited states is difficult, since the known values<sup>[8-10]</sup> for several levels differ greatly and, in addition, the levels with  $n > 3$  have not been calculated. In particular, the intense line 16 is apparently due to the transition  $3d_{-2} - 4f_{-3}$ , inasmuch as when  $H$  is decreased the energy of this line tends to the value 0.27 meV, which is close to the energy of the transition between the levels  $n=3$  and  $n=4$  at  $H=0$ , and in a field  $H=60 \text{ kOe}$  the  $3d_{-2}$  level has, under equilibrium conditions, a much larger population than the other levels with  $n=3$ . This identification is confirmed also by the fact that this line is realized in the spectrum when the radiation has left-hand circular polarization and propagates in the  $H$  direction.

Measurement results that are analogous in many respects were recently published in the extensive paper of Simmonds *et al.*<sup>[7]</sup> In particular, for donors in GaAs, using a laser with  $\lambda = 337 \mu$ , four lines were obtained, whereas at  $\lambda = 311 \mu$  one line was obtained in the spectrum of the transition between the excited states. The position of the line  $B_2$  ( $2p_{-1} - 2s$ )<sup>[7]</sup> coincided in this case with that of our line 3 ( $2p_{-1} - 2s$ ), while the position of the line  $A_1$  (identified in<sup>[7]</sup> as  $2s - 3p_{+1}$ ) coincided with that of our line 11 ( $2p_0 - 3d_{+1}$ ). We were unable to observe the line designated X in<sup>[7]</sup>, while the line  $A_2$  (identified as  $2p_0 - 3d_{+1}$ ) differs substantially in its spectral position from the line 13 (we did not observe any other lines in the spectrum at  $\lambda = 337 \mu$ ). To trace the dependence of the line energy on  $H$ , in view of the very limited tuning range of the laser used in<sup>[7]</sup>, the following procedure was used; We registered the spectra of the donors not only in GaAs, but also in InP, CdTe, and CdSe. The spectra of the donors in different semiconductors, measured at the same wavelength, fall in different regions of the dimensionless  $\epsilon/\text{Ry}^* - \gamma$  diagram, since all are described by the same Hamiltonian (1). This method yielded<sup>[7]</sup> results close to those given here for several lines, as well as results that differ. For example, a comparison of the spectrum of  $n$ -CdTe at  $\lambda = 337 \mu$ , which has the most lines, with our spectrum of  $n$ -GaAs at  $\lambda = 790 \mu$ , which is equivalent to it on the dimensionless diagram, shows that the energies of the lines  $A_2$  ( $2p_0 - 3d_{+1}$ ) and  $B_1$  ( $2p_{-1} - 3d_{+1}$ ) exceed the energies of the corresponding lines 11 and 10 by only 0.08 meV, apparently because of the small inaccuracy in the value of  $\text{Ry}^*$  for the donors in CdTe. The positions of the lines  $A_1$  ( $2s - 3p_{+1}$ ) and  $B_2$  ( $2p_{-1} - 2s$ ) differ from those of lines 12 and 3 much more, this being apparently due to the central-bin correction for the 2s level of the CdTe donors. The lines C, D, E, F, and G cannot be compared with the lines 4, 5, 9, 13, and 14 of the discussed GaAs spectrum. Consequently, a reliable interpretation of the experimental results with the aid of a comparison of the spectra of the donors of different semiconductors calls for additional experiments to be performed for a number of lines.

4. We were unable to identify lines 9 and 13 with transitions between excited states of donors, despite the large volume of the corresponding experimental data. They can be the most intense lines in the spec-

trum. They can be measured starting with  $H = 300$  Oe near an energy  $0.8$  meV ( $0.14$  Ry\*), i. e., at  $H = 0$  these lines are close to the transition from  $n = 2$  to  $n = 3$  in the hydrogenlike spectrum. In addition, in the entire  $H$  interval where both lines fall in the employed range of waves, the difference of their energies amounts to  $\hbar\omega_{st}$ . Therefore they can correspond only to the following allowed transitions between the hydrogen-like levels;  $2s - 3p_{\pm 1}$ ,  $2p_0 - 3d_{\pm 1}$ ,  $2p_{\pm 1} - 3d_{\pm 2}$ ,  $2p_{\pm 1} - 3d_0$ , and  $2p_{\pm 1} - 3s$ . However, the first three are realized also for other spectral lines. The energies of the remaining two transitions differ substantially from the positions of the lines 9 and 13, and have different values in calculations by different authors (owing to the positions of  $3s$  and  $3d_0$ ). In addition, in a sufficiently strong field  $H$ , at  $T = 2^\circ\text{K}$ , the  $2p_{\pm 1}$  level is not populated under equilibrium conditions: this manifests itself in experiment, for example, by the fact that it is impossible to observe the transition  $2p_{\pm 1} - 3d_{\pm 2}$ , whose energy exceeds that of the  $2p_{\pm 1} - 3d_{\pm 2}$  line (line 6) by  $\hbar\omega_{st}$ . It is interesting that the intensities of the lines in question, in contrast to those of the others, decrease with aging of the samples: since the time of publication of our preceding paper<sup>[17]</sup> it has decreased by approximately two orders of magnitude. The foregoing evidence, as well as the much larger width ( $\sim 0.3$  meV) of these lines, suggests that they do not belong to the spectrum of a single neutral donor, but, for example, to donor pairs.<sup>[23]</sup>

#### Donors in Ge

1. The spectrum of the donors in Ge is much more complicated than in GaAs, and the levels are degenerate only in  $|m|$ . To identify the corresponding Zeeman components, however, it suffices to determine the lines of the transitions between excited states at  $H = 0$ , by using Faulkner's theory.<sup>[24]</sup> The influence of a sufficiently strong magnetic field on the donor spectrum in Ge (in the present study, in contrast to the earlier work,<sup>[11]</sup> it is investigated, just as in GaAs, up to  $H \approx 60$  kOe) is more complicated also because of the strong effective-mass anisotropy and the fact that the conduction band has many valleys. The abundance of

TABLE II. Energy and identification of some of the observed photoconductivity lines of Ge (Sb) and of the excited levels.

Line number	$\epsilon$ of line, meV	Identification	Level	$\epsilon$ of level, meV	
				Experiment	Calculation <sup>[24]</sup>
1	0.74	$3d_0 \rightarrow 4p_{\pm 1}$	$2p_0$	4.75	4.74
2	0.82	$4p_0 \rightarrow 4d_{\pm 1}$	$2s$	3.60	3.52
3	0.9	$3d_0 \rightarrow 4f_{\pm 1}$	$3p_0$	2.56	2.56
4	1.31	$3p_0 \rightarrow 3d_{\pm 1}$	$2p_{\pm 1}$	1.73	1.73
5	1.03*	$2s \rightarrow 3p_0$	$4p_0$	1.67	1.67
6	1.87	$2s \rightarrow 2p_{\pm 1}$	$3d_0$	4.48	1.34
7	2.57	$2s \rightarrow 3p_{\pm 1}$	$3d_{\pm 1}$	1.25	—
8	2.86	$2s \rightarrow 4p_{\pm 1}$	$3p_{\pm 1}$	1.03	1.03
9	3.02	$2s \rightarrow 4f_{\pm 1}$	$4d_{\pm 1}$	0.85	—
10	1.16	$2p_0 \rightarrow 2s$	$4p_{\pm 1}$	0.74	0.73
11	3.27*	$2p_0 \rightarrow 3d_0$	$4f_{\pm 1}$	0.58	0.61
12	3.50	$2p_0 \rightarrow 3d_{\pm 1}$	$5d_{\pm 1}$	0.63	—
13	3.90	$2p_0 \rightarrow 4d_{\pm 1}$	$5g_{\pm 1}$	0.51	—
14	4.12	$2p_0 \rightarrow 5d_{\pm 1}$			
15	4.24	$2p_0 \rightarrow 5g_{\pm 1}$			

\*This line is not observed in the absence of  $H$ , and the energy was obtained by extrapolation of its Zeeman components.

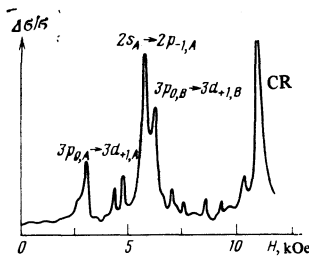


FIG. 4. Photoconductivity spectrum of Ge (Sb),  $\lambda = 786 \mu$ ,  $T = 8$  K,  $\mathbf{H} \parallel [111]$ .

lines in the spectra makes it difficult to determine the energy spectrum of the donors in as large a volume as possible, we have therefore attempted to confine the measurements mainly to those lines which are needed to determine the dependence of the energy on  $H$  for five of the lowest excited levels in five orientations of  $\mathbf{H}$  (A to E). These are the lines of the transitions  $2s - 3p_0$ ,  $3p_0 - 3d_{-1}$ ,  $2p_0 - 2s$ ,  $2s - 2p_{-1}$  and  $2p_0 - 3d_{-1}$ , in which the levels  $2p_0$ ,  $2s$ ,  $3p_0$ , and  $2p_{-1}$  have been calculated<sup>[11,13]</sup> in a broad interval of  $H$ , and the level  $3d_{-1}$  can be easily determined in experiment. The designations of the levels in a magnetic field are here the same at  $H = 0$ . If the chosen lines have a low intensity or a complicated dependence of the energy on  $H$  in certain segments, then it becomes necessary, for a reliable measurement in a wide range of  $H$ , to register a large number of additional lines close in position in the spectrum to the chosen lines. Table II lists the energies of the required spectral lines of the photoconductivity at  $H = 0$  and their identification, which will be discussed after describing the results of the experiment.

2. Figure 4 shows by way of example a segment of the spectrum, at  $\lambda = 786 \mu$ , of the photoconductivity of Ge with  $N_d = 2 \times 10^{13} \text{ cm}^{-3}$  (Sb) and  $N_a = 2 \times 10^{12} \text{ cm}^{-3}$  at  $T = 8^\circ\text{K}$  and  $\mathbf{H} \parallel [111]$ . A large number of Zeeman components of photothermal ionization lines of the excited states of the shallow donors and the CR line of the free electrons are observed. Figure 5 gives the dependence of the energies of the three most intense lines (in the absence of  $H$ ) of the spectrum,  $2p_0 - 3d_{\pm 1}$ ,  $2s - 2p_{\pm 1}$ , and  $3p_0 - 3d_{\pm 1}$ , on the value of the magnetic field in the same orientation ( $\mathbf{H} \parallel [111]$ ) as the spectrum of Fig. 4, in the entire investigated range. The pair of the external Zeeman components of each line corresponds here to the orientation A, while the pair of the internal components to orientation B of the field  $\mathbf{H}$ . At low energies ( $\epsilon = 0.6 - 0.8$  meV) the intensities of the lines of the transitions  $2s - 2p_{-1}$  and  $3p_0 - 3d_{-1}$  decrease so much

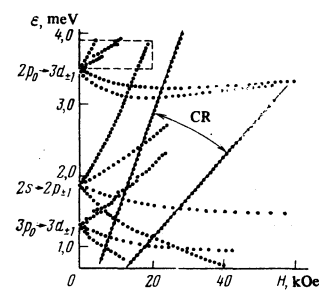


FIG. 5. Dependence of the energy on  $H$  for three lines of the spectrum of Ge (Sb), ( $\mathbf{H} \parallel [111]$ ).

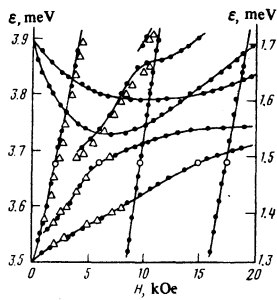


FIG. 6. Plot of  $\varepsilon(H)$  of the Ge (Sb) lines for two sections of the spectrum,  $\mathbf{H} \parallel [111]$ : ●—lines of the range  $\varepsilon = 3.5\text{--}3.9$  meV;  $\Delta$ —lines of the range  $\varepsilon = 1.3\text{--}1.7$  meV; ○—results of [6] for  $\varepsilon = 3.68$  meV.

that they can no longer be observed against the background of other spectral lines, the number of which is large. The abundance of lines causes the weakest lines to be resolved only on individual segments of the spectrum and it becomes impossible to trace the dependence of their energy on  $H$  in a wide range. This, however, is not necessary, since measurement of only the most intense lines, as will be clear from the following, yields sufficiently detailed information on the spectrum of the donors in a magnetic field. The succeeding plots therefore show the results of measurements made on sufficiently intense lines.

Figure 6 reveals a characteristic singularity inherent in the Zeeman spectrum of the excited states of donors, namely, a complicated dependence of the line energy on  $H$  and almost full coincidence of all the singularities of  $\varepsilon(H)$  for certain lines, for example,  $2p_0 - 3d_{+1}$  and  $3p_0 - 3d_{+1}$ . The figure shows also, in a different scale, the upper dashed rectangle of Fig. 5, the experimental data of which are designated by dark points, as well as the results of measurements of the  $3p_0 - 3d_{+1}$  line (marked by triangles), which is made to coincide at  $H = 0$  with the line  $2p_0 - 3d_{+1}$ .

3. The smallest number of Zeeman components is observed at  $\mathbf{H} \parallel [100]$ , so that the real resolution of the lines in the spectra is higher than in other orientations of  $\mathbf{H}$ , and it is easier here to obtain more complete data on the dependence of the line energy on  $\mathbf{H}$ . Figure 7 shows the results of the measurements for the components of the lines  $2s - 2p_{+1}$ ,  $2s - 3p_{+1}$ ,  $2p_0 - 3d_{+1}$ , and for a number of others in the range  $\varepsilon = 2.9\text{--}3.9$  meV. Figure 8 illustrates the unusual behavior of the intensity of the Zeeman components at the place where there are

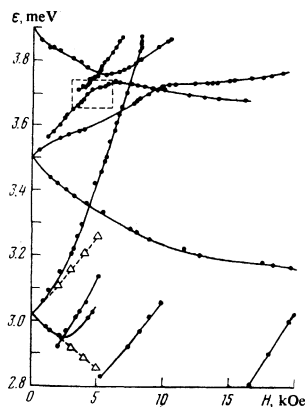


FIG. 7. The energies (in the range  $\varepsilon = 2.8\text{--}3.9$  meV) of several spectral lines of Ge (Sb) vs.  $H$  ( $\mathbf{H} \parallel [100]$ ). ●—experimental data,  $\Delta$ —sum of the energies of the Zeeman components of the lines  $2p_0 - 2s$  and  $2s - 2p_{+1}$ .

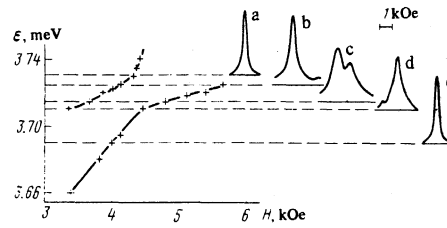


FIG. 8. The boxed region of Fig. 7, and the photoconductivity-spectrum sections recorded with  $H$  scanned and the radiation energies fixed.

singularities in the  $\varepsilon(H)$  dependences of the spectral lines. It shows to a large scale the segment in the small box in Fig. 7, and gives the photoconductivity lines  $\Delta\sigma/\sigma = f(H)$  (a to e) recorded at the values of  $\varepsilon$  indicated by the dashed lines. It is seen that even in a small range of values of  $\varepsilon$  and  $H$  the line intensity changes significantly. The spectra a and e reveal only one line each, just as outside the singularity region, while the intermediate spectra (b–d) show a rapid redistribution of the intensity among the lines. The broadening of the lines b–d in comparison with a and e is due only to the appreciable decrease of the slope of the  $\varepsilon(H)$  plot, whereas the line width remains unchanged in the case of frequency scanning and fixed  $H$ .

4. Figure 9 shows the results of measurements of  $\varepsilon(H)$  of three spectral lines ( $2s - 2p_{+1}$ ,  $2p_0 - 3d_0$  and  $2p_0 - 3d_{+1}$ ) at  $\mathbf{H} \parallel [110]$ ; it shows only the components for which the magnetic field is perpendicular to the symmetry axis of the constant-energy ellipsoid (the orientation E). It is seen that for the lines  $2s - 2p_{+1}$  and  $2p_0 - 3d_{+1}$  the splitting becomes noticeable starting with  $H = 2\text{--}4$  kOe. The obtained splitting of two levels ( $2p_{+1}$  and  $3d_{+1}$ ) depends nonlinearly on  $H$  (this dependence is even nonmonotonic for the level  $3d_{+1}$ ) and reaches values  $0.15\text{--}0.3$  meV at  $H = 40\text{--}50$  kOe.

Only one component is revealed for the line  $2p_0 - 3d_0$  at  $\mathbf{H} \parallel [110]$ . Its measurement with the sample rotated in such a way that  $\mathbf{H}$  remains in the (110) plane has shown that the energy of this component changes little, and the minimum energy gap (in the measured range of  $H$ ) between this line and the component of the line  $2p_0 - 3d_{+1}$  closest to it in energy decreases, amounting to  $\approx 0.01$  meV, when the angle between  $\mathbf{H}$  and  $[110]$  reaches  $25^\circ$ . The range of  $H$  in which the line  $2p_0 - 3d_0$  has an intensity high enough to be measured decreases substantially, and it cannot be resolved in the spectrum when the angle is increased further.

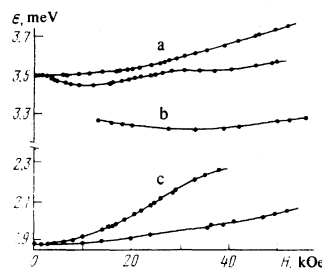


FIG. 9. Plot of  $\varepsilon(H)$  for the Zeeman components of: a— $2p_{0,E} - 3d_{+1,E}$ , b— $2p_{0,E} - 3d_{0,E}$  and c— $2s_E - 2p_{+1,E}$  in Ge(Sb).

TABLE III. Energies (meV) of transitions\* between excited states of the donors in Ge in a magnetic field.

H, kOe	$2p_0 \rightarrow 3d_{-1}$					$3p_0 \rightarrow 3d_{-1}$				
	A	B	C	D	E	A	B	C	D	E
2	3.380	3.453	3.430	3.403	3.490	1.187	1.261	1.242	1.084	1.31
4	3.293	3.406	3.361	3.333	3.470	1.090	1.218	1.185	1.108	1.293
6	3.240	3.372	3.314	3.277	3.458	1.020	1.179	1.128	1.053	1.277
8	3.197	3.343	3.271	3.240	3.449	0.954	1.144	1.078	1.000	1.267
10	3.168	3.315	3.241	3.200	3.444	0.905	1.117	1.028	0.952	1.256
15	3.11	3.273	3.192	3.145	3.456	---	1.070	0.955	0.849	1.262
20	3.11	3.256	3.175	3.137	3.488	---	---	0.900	---	---
25	3.122	3.25	3.175	3.152	3.500	---	1.001	0.863	---	---
30	3.148	3.25	3.185	3.190	3.522	---	0.984	0.839	---	---
35	3.178	3.261	3.216	3.255	3.522	---	0.968	0.833	---	---
40	3.213	3.273	3.246	3.328	3.530	---	0.957	0.846	---	1.260
45	3.244	3.288	3.282	3.411	3.547	---	---	0.870	---	1.269
50	3.272	3.311	3.333	3.494	3.567	---	---	0.905	---	1.278
55	3.306	3.334	3.385	---	3.583	---	---	---	---	---

H, kOe	$2p_0 \rightarrow 3d_{+1}$					$3p_0 \rightarrow 3d_{+1}$				
	A	B	C	D	E	A	B	C	D	E
2	3.664	5.573 <sup>1)</sup>	3.630 <sup>1)</sup>	3.613 <sup>1)</sup>	3.50	1.467	1.385 <sup>1)</sup>	1.410 <sup>1)</sup>	1.448	1.31
4	3.863	3.627 <sup>1)</sup>	3.690 <sup>2)</sup>	3.788 <sup>2)</sup>	3.50	1.663	1.439 <sup>1)</sup>	1.502 <sup>2)</sup>	1.590	1.31
6	4.07	3.734 <sup>2)</sup>	3.827 <sup>2)</sup>	---	3.50	1.871	1.537 <sup>2)</sup>	1.627 <sup>2)</sup>	1.761	1.31
8	4.31	3.800 <sup>2)</sup>	---	---	3.50	2.120	1.601 <sup>2)</sup>	1.745 <sup>2)</sup>	1.940	1.31
10	4.55	3.892 <sup>2)</sup>	---	---	3.503	2.327	1.651 <sup>2)</sup>	1.880 <sup>2)</sup>	2.134	1.31
15	---	---	---	---	3.515	---	1.893 <sup>3)</sup>	2.229 <sup>2)</sup>	2.604	1.32
20	---	---	---	---	3.529	---	2.138 <sup>3)</sup>	2.595 <sup>2)</sup>	---	1.332
25	---	---	---	---	3.556	---	---	---	---	1.351
35	---	---	---	---	3.622	---	---	---	---	1.384
50	---	---	---	---	3.748	---	---	---	---	1.455

H, kOe	$2s \rightarrow 2p_{-1}$					$2s \rightarrow 2p_{+1}$				
	A	B	C	D	E	A	B	C	D	E
2	1.755	1.835	1.242	1.776	1.87	2.027	1.920	1.958	2.12	1.87
4	1.650	1.795	1.185	1.677	1.872	2.201	1.980	2.057	2.155	1.880
6	1.550	1.758	1.128	1.600	1.876	2.380	2.037	2.161	2.292	1.887
8	1.468	1.725	1.078	1.541	1.880	2.566	2.103	2.263	2.444	1.902
10	1.395	1.690	1.028	1.488	1.884	2.753	2.172	2.380	2.619	1.923
15	---	1.625	0.955	1.354	1.890	3.367	2.352	2.695	---	1.963
20	1.144	1.585	0.900	1.220	1.911	3.94	2.543	3.02	---	2.026
25	1.040	1.560	0.863	---	1.926	4.56	---	3.385	---	2.098
30	0.950	1.537	0.839	---	1.946	---	---	---	---	2.170
35	---	1.520	0.833	---	1.965	---	---	---	---	2.233
40	0.786	1.507	0.846	---	1.989	---	---	---	---	---
45	---	1.595	0.870	---	2.012	---	---	---	---	---
50	---	1.489	0.905	---	2.037	---	---	---	---	---
55	---	1.482	---	---	---	---	---	---	---	---

H, kOe	$2p_0 \rightarrow 2s$					$2s \rightarrow 3p_0$				
	A	B	C	D	E	A	B	C	D	E
15	---	---	---	---	---	---	---	1.045	---	---
20	---	---	1.217	---	---	---	---	1.061	---	---
25	1.237	1.210	1.243	---	---	1.114	---	1.069	---	---
30	1.260	1.224	1.273	---	---	1.129	1.034	1.080	---	---
35	1.286	1.242	1.301	---	---	1.142	1.039	1.081	---	---
40	1.316	1.262	1.332	---	---	1.157	1.043	1.073	---	---
45	1.343	1.283	1.364	---	---	1.174	1.050	1.060	---	---
50	1.372	1.304	1.395	---	---	1.194	1.054	1.041	---	---
55	1.390	1.327	1.428	---	---	1.211	1.059	1.020	---	---
60	1.438	1.349	1.460	---	---	---	1.064	---	---	---

\*The number in the superscript indicates the number of anticrossings corresponding to the given transition energy.

Table III, which summarizes the presented experimental results, shows the values of the energies of the Zeeman components selected by us for a detailed analysis of the five transitions between excited states of the donors in Ge at five orientations of H (A-E).

5. The interpretation of the experimental data and their comparison with theory calls for reliable identification of the spectral lines. The results of this identification for some of the lines are given in the left side of Table II; the right side of this table contains the level energies together with the corresponding theoretical values.<sup>[24]</sup> To calculate the energy of the excited states, the calculations are normalized to the energy of one level (in this case  $2p_{\pm 1}$ ). It is seen that the experiment yields line series that have a common lower level (for

example,  $2p_0$  or  $2s$ ) and different upper levels. The energies of all the levels of the series of transitions from  $2s$  turn out to be close to those calculated.

In addition to the energy position and the regularities in the series, appreciable information needed for line identification is provided by measurements in a wide range of H. Let us consider by way of example the identification, at  $H=0$ , of lines with energies 3.5, 1.31, 1.16, and 1.03 meV. Even in a weak magnetic field ( $H = 100 - 300$  Oe) it becomes clear that for the first two transitions  $m$  changes by  $\pm 1$ , and for the two other transitions it remains unchanged (the 3.5 and 1.31 meV lines are split, unlike the 1.16 and 1.03 meV lines). The energy of the first transition is so large that the starting level for it can be only the first excited level. This is confirmed also by the fact that all the lines of the series of transitions from the first excited state have the same energy shift when the spectra of various shallow donors (Sb, P, As) are compared.<sup>[11]</sup> The energy position of the level  $2p_0$  (4.75 meV) for the transitions  $2p_0 - 2s$  and  $2s - 2p_{\pm 1}$  (see also below concerning the identification of these lines). The final state of the most intense line of the spectrum (3.5 meV) has in this case an energy 1.25 meV (this is the  $3d_{\pm 1}$  level). The agreement between the complicated H-dependences of the energies of the 3.5 and 1.31 meV lines (Fig. 6) is evidence that these lines have a common  $3d_{\pm 1}$  state. The energy of the starting state of the 1.31 meV line should in this case amount to 2.56 meV, i.e., this is the  $3p_0$  state. The two lines (1.16 and 1.03 meV) with  $\Delta m = 0$  are shifted very little in the magnetic field, because the corresponding transitions take place between low-lying levels. At the same time, the sum of the energies of the corresponding Zeeman components of these lines agrees within the experimental accuracy with the difference of the energies of the components of the transitions  $2p_0 - 3d_{-1}$  and  $3p_0 - 3d_{-1}$  (meV) in a wide range of fields H:

$$\begin{aligned}
 H, \text{ kOe:} & & 20 & 25 & 30 & 35 & 40 & 45 & 50 \\
 \epsilon(2p_{0,C} \rightarrow 3d_{-1,C}) - \epsilon(3p_{0,C} \rightarrow 3d_{-1,C}): & & 2.275 & 2.312 & 2.347 & 2.383 & 2.400 & 2.412 & 2.428 \\
 \epsilon(2p_{0,C} \rightarrow 2s_C) + \epsilon(2s_C \rightarrow 3p_{0,C}): & & 2.278 & 2.312 & 2.353 & 2.382 & 2.405 & 2.424 & 2.436
 \end{aligned}$$

Between the levels  $2p_0$  and  $3p_0$ , however, there is located only the level  $2s$  with energy 3.60 meV, calculated from the position of the 1.87-meV line ( $2s - 2p_{\pm 1}$ ). These two lines are therefore unambiguously identified with the 1.16 and 1.03 meV lines corresponding to  $2p_0 - 2s$  and  $2s - 3p_0$ , respectively.

Lee, Larsen, and Lax<sup>[11]</sup> have cast doubts on the correctness of our identification<sup>[11]</sup> of the lines with energies 1.87 and 1.16 meV (the transitions  $2s - 2p_{\pm 1}$  and  $2p_0 - 2s$ ), since our experiments did not reveal the valleys—the orbital splitting of the  $2s$  level (0.069 meV), which they calculated<sup>[11]</sup> for Sb and Ge. This fact is discussed in<sup>[25]</sup> where it is shown that in the absorption spectrum of Ge (Sb), in contrast to the photoconductivity spectrum, splitting of the  $2s$  level is observed and amounts to  $0.03 \pm 0.01$  meV. The  $2s$ -level splitting observed in the photoconductivity spectrum of Ge (P) is  $0.28 \pm 0.01$  meV, and in Ge (As) its value is  $0.4 \pm 0.01$  meV. The weak line with energy 3.02 meV was identified by us earlier<sup>[11]</sup> from its energy position in the



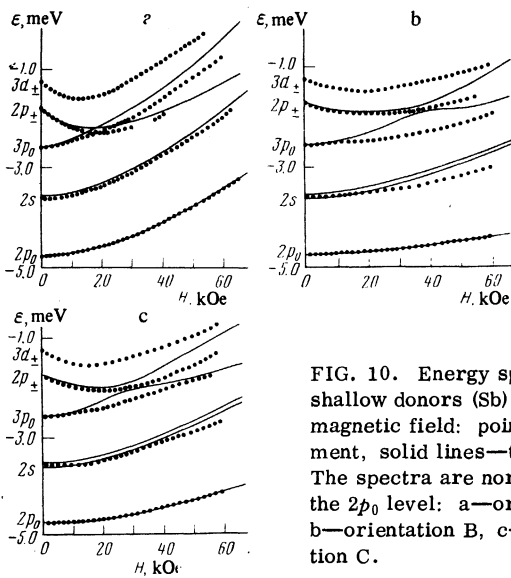


FIG. 10. Energy spectrum of shallow donors (Sb) in Ge in a magnetic field: points—experiment, solid lines—theory.<sup>[11,13]</sup> The spectra are normalized to the  $2p_0$  level: a—orientation A, b—orientation B, c—orientation C.

spectrum as the transition  $2p_0 - 2p_{\pm 1}$ . From the data of Fig. 7, however, which shows (triangles) for the transition  $2p_0 - 2p_{\pm 1}$  at  $\mathbf{H} \parallel [100]$  a splitting equal to the sum of the corresponding Zeeman components of the lines  $2p_0 - 2s$  and  $2s - 2p_{\pm 1}$ , it is seen that the behavior of the 3.02 meV line in a magnetic field differs substantially from the predicted relation. The large transition energy and the strong quadratic shift of the components of this line in the field  $H$  indicates that this is a transition from the  $2s$  level to a relatively high excited state with energy 0.58 meV, apparently into  $4f_{\pm 1}$ .

6. The foregoing identification of the lines yields the energy spectrum of the donors in the entire investigated magnetic-field interval, from the experimental data gathered in Table III. To this end, the  $H$ -dependence of the energy of one of the levels of the spectrum, just as in the case  $H = 0$ , must be normalized to the theoretical value. Since the results of even the latest calculations of the donor levels in Ge<sup>[11,13]</sup> differ noticeably from our data (see Fig. 10), a wrong normalization to the calculation can introduce a noticeable error in the absolute values of the energies of all the remaining levels, even though at any value of  $H$  the energy gaps between arbitrary levels, remain, of course, unchanged. We have chosen for the normalization the  $2p_0$  level, since, first, the energy gap between this level and any other level remains appreciable in the entire employed interval of  $H$  and, second, this is the lowest level of this symmetry. Its energy position is least influenced by admixture of other states, so that the calculation of this level is apparently the most accurate. Figure 10 shows five levels of the energy spectrum, constructed in this manner, for three orientations of  $\mathbf{H}$  (A, B, C). It is seen that the best agreement with theory is in the orientation A, namely, the energies of the levels  $2p_{-1}$  and  $2s$  differ from the calculated values by not more than 0.08 meV in the entire range of  $H$ . It should be noted that this difference is still smaller by almost one order of magnitude than the experimental error. For the  $3p_0$  level the difference is appreciable

also in this orientation and reaches 0.2 and 0.4 meV respectively at  $H = 30$  and 60 kOe. In the orientations B and C, the calculation agrees less with the experimental energy spectrum. The discrepancy for the  $3p_0$  level leads to poor agreement also for the  $2p_{-1}$  level in the region of their strong interaction, whereas far from this region the results of the calculations and of the experiment for one of the levels are close (in the C orientation this corresponds to  $H \lesssim 30$  kOe and  $H \gtrsim 50$  kOe). The smallest energy gap between the levels  $2p_{-1}$  and  $3p_0$  in the orientation C amounts to 0.20 meV (at  $H \approx 35$  kOe); calculation<sup>[13]</sup> yields for this gap 0.08 meV at  $H = 25$  kOe. In the orientation B, the agreement for the region of interaction of the levels  $2p_{-1}$  and  $3p_0$  is worse: experiment yields a minimum gap of 0.42 meV in a field  $H = 55$  kOe, while calculation yields 0.12 meV at  $H = 35$  kOe.

7. We discuss now the singularities noted in Secs. 2–4 of the Zeeman spectrum of the donors in Ge, and compare the results with the published experimental data. Horii and Nisida<sup>[4]</sup> investigated the absorption of the radiation that induces transitions from the ground to the excited  $p$  states of antimony and arsenic in germanium. Since the starting states of the transitions were different in our experiments from those of<sup>[4]</sup>, it is impossible to compare the data directly. Figure 11 shows plots of the energy differences of the levels  $2p_0$  and  $2p_{\pm 1,A}$ ,  $2p_{\pm 1,B}$ ,  $3p_{0,B}$  in accordance with the data of Horii and Nisida<sup>[4]</sup> and in accordance with Fig. 10. It is seen that they agree within the limits of the resolution of the spectrometer (0.06 meV)<sup>[28,41]</sup> for the levels  $2p_{\pm 1,B}$  and  $3p_{0,B}$  in the entire range of  $H$ , and for level  $2p_{-1,A}$  only up to 28 kOe (beyond this, the  $1s - 2p_{-1,A}$  line was measured in<sup>[4]</sup> at only one point,  $H = 46$  kOe).

Muro and Nisida<sup>[6]</sup> measured the photoconductivity spectrum using a laser at  $\lambda = 337 \mu$ . Their results up to  $H = 20$  kOe are marked in Fig. 6 by circles, and it is seen that the positions of all the spectral lines agree with our data.

To our knowledge, no measurements in Ge in the D and E orientations have been made so far. Yet the E orientation is of interest from the point of view of the behavior of the levels when  $\mathbf{H}$  is perpendicular to the symmetry axis of the constant-energy ellipsoid of the conduction band, when the levels with  $m = \pm 1$  should not split in the weak-field approximation.<sup>[27]</sup> The quadratic Zeeman shift of the  $2p_{\pm 1}$  level was investigated in Si at

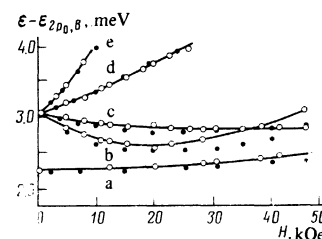


FIG. 11. Plots of the energy differences of the levels  $2p_{0,B}$  and  $3p_{0,B}$  (a),  $2p_{0,B}$  and  $2p_{-1,A}$  (b),  $2p_{0,B}$  and  $2p_{-1,B}$  (c),  $2p_{0,B}$  and  $2p_{+1,B}$  (d),  $2p_{0,B}$  and  $2p_{+1,A}$  (e), in accordance with the experimental data of Fig. 10 (●) and of<sup>[5]</sup> (○).

this orientation of  $\mathbf{H}$  up to  $H \gtrsim 60$  kOe<sup>[5]</sup> and no splitting was observed. It should be noted that the same workers assumed, in a preceding paper,<sup>[28]</sup> the splitting of the corresponding level to be small. The results of our experiment on Ge (Fig. 9), however, show that the levels with  $m = \pm 1$  can be split starting with  $H = 2-4$  kOe because of their interaction. The splitting can exceed the quadratic level shift.

Let us illustrate the influence of the magnetic field on the doubly degenerate level with  $m = \pm 1$ . The Hamiltonian (2) in the E orientation is of the form

$$\mathcal{H} = \mathcal{H}_0 + V = \mathcal{H}_0 + \mathcal{H}_1 + \mathcal{H}_2 + \mathcal{H}_3 + \mathcal{H}_4,$$

where  $\mathcal{H}_0$  is the Hamiltonian of the unperturbed neutral donor,

$$\mathcal{H}_1 = \frac{i\gamma z}{2} \frac{\partial}{\partial z}, \quad \mathcal{H}_2 = -\frac{i\gamma}{2} \delta y \frac{\partial}{\partial z}, \quad \mathcal{H}_3 = \frac{\gamma^2}{16} z^2, \quad \mathcal{H}_4 = \delta \frac{\gamma^2}{16} y^2$$

(in dimensionless units),  $\delta = m_{\perp}/m_{\parallel}$ , the  $z$  axis coincides with the symmetry axis of the constant-energy ellipsoid, and  $\mathbf{H} \parallel x$ .

Choosing the wave function without the magnetic field in the form  $\Psi_m = f(\rho, z) e^{im\phi}$ , we obtain

$$\begin{aligned} \langle \Psi_{+1} | V | \Psi_{+1} \rangle &= \langle \Psi_{-1} | V | \Psi_{-1} \rangle, & \langle \Psi_m | \mathcal{H}_1 + \mathcal{H}_2 | \Psi_m \rangle &= 0, \\ \langle \Psi_m | \mathcal{H}_1 + \mathcal{H}_2 + \mathcal{H}_3 | \Psi_{-m} \rangle &= 0, & \langle \Psi_m | \mathcal{H}_3 + \mathcal{H}_4 | \Psi_m \rangle &= a\gamma^2, \\ \langle \Psi_m | \mathcal{H}_1 | \Psi_{-m} \rangle &= b\gamma^2. \end{aligned}$$

Here  $a$  and  $b$  are constants. Using first-order perturbation theory for the degenerate states,<sup>[29]</sup> we have the dependence of the energy of the states on the magnetic field:  $\varepsilon_{\pm} = \varepsilon_0 + (a \pm b)\gamma^2$ , where  $\varepsilon_0$  is the level position at  $H = 0$ . The wave functions of the two states are of the form  $\Phi_{\pm} = 2^{-1/2}(\Psi_{\pm 1} \pm \Psi_{-1})$ . A similar quadratic splitting was observed by us for the transition line  $2s - 2p_{\pm 1}$  in the orientation E (Fig. 9).

It is possible to take into account the influence of the state with  $m = 0$  and with the same parity by introducing for this state the wave function  $\Psi_0 = g(\rho, z)$  at  $H = 0$ . From the symmetry of the wave functions we obtain  $\langle \Phi_{\pm} | V | \Psi_0 \rangle = 0$ , but  $\langle \Phi_{\pm} | \hat{V} | \Psi_0 \rangle \neq 0$ , i. e., the function  $\varepsilon_{\pm}(H)$  remains unperturbed, while  $\varepsilon_-(H)$  can be quite complicated. This agrees with the data of Fig. 9 for the line  $2p_0 - 3d_{\pm 1}$ . The behavior of the lower component of this line (corresponding to  $\varepsilon_-(H)$ ) can be attributed to the influence of two levels with  $m = 0$  that are close to  $3d_{\pm 1}$  ( $3d_0$  and  $4s$ ).

We now examine in greater detail the singularities of the Zeeman spectra shown in Figs. 5-8. They manifest themselves in a qualitative difference between the behaviors of the Zeeman components of the levels for the A orientation of the magnetic field and for arbitrary other orientations, in which  $\mathbf{H}$  makes an angle with the symmetry axis of the conduction-band ellipsoid. The energy of the former varies smoothly with the magnetic field, while for the latter abrupt changes of the line intensities and of the slope of the  $\varepsilon(H)$  plots are observed. The reason is that the states in the spectrum of the donors in the A orientation are characterized by a definite value of  $m$ , and levels with different  $m$  can intersect as  $\mathbf{H}$  is varied. At all other orientations, a magnetic-field

component perpendicular to the axis of the heavy mass appears and mixes these states<sup>[13]</sup>; this leads to anti-crossing of the levels.

The interaction of the levels of a shallow impurity in the magnetic field was observed also earlier (for example,<sup>[30,31]</sup>) but the insufficient spectral resolution did not make it possible to investigate it in detail. It is seen from the figures that the interacting levels are fully resolved here when the minimum energy gap between them reaches  $\approx 0.01$  meV. In addition, in contrast to earlier studies, the spectra reveal clearly interactions not only between levels to which intense optical transitions take place (for example,  $2p_{-1}$  and  $3p_0$ ), but between levels such that the transition to one of the interacting levels appears at all in the A orientation, but when states with different  $m$  are mixed in a narrow range of energies near the region of the strong interaction the transition intensity becomes appreciable. An example of the last case can be the interaction of the  $3d_{+1}$  level consecutively with five high-lying levels (Fig. 5), a fact reflected in the dependence of the energy and of the intensity on  $H$  for the  $2p_0 - 3d_{+1}$  transition as well as for  $3p_0 - 3d_{+1}$  (Figs. 6 and 8).

It is possible to explain in this manner also the appearance in the spectrum,<sup>[6]</sup> at  $\lambda = 337 \mu$ , of a line at  $H = 15$  kOe for the B orientation, although no corresponding Zeeman component is observed in the A orientation. It is seen from Fig. 6 that the discussed line manifests itself in the spectrum at  $H \gtrsim 2$  kOe in the region of the anticrossing of the level  $3d_{\pm 1}$  with one of the lower lying levels.

- <sup>1</sup>E. M. Gershenson, G. N. Gol'tsman, and N. G. Ptitsina, Zh. Eksp. Teor. Fiz. **64**, 587 (1973) [Sov. Phys. JETP **37**, 299 (1973)].
- <sup>2</sup>S. D. Seccombe and D. M. Korn, Solid State Commun. **11**, 1539 (1972); M. S. Skolnic, L. Eaves, R. A. Stradling, J. C. Portal, and S. Askenazy, Solid State Commun. **15**, 1403 (1974).
- <sup>3</sup>E. E. Haller and W. L. Hansen, Solid State Commun. **15**, 687 (1974).
- <sup>4</sup>K. Horii and Y. Nisida, J. Phys. Soc. Jpn. **31**, 783 (1971).
- <sup>5</sup>G. Taravella, Ph. Arcas, and B. Pajot, Solid State Commun. **13**, 353 (1973).
- <sup>6</sup>K. Muro and Y. Nisida, J. Phys. Soc. Jpn. **34**, 563 (1973).
- <sup>7</sup>P. E. Simmonds, J. M. Chamberlain, R. A. Hoults, R. A. Stradling, and C. C. Bradley, J. Phys. C **7**, 4164 (1974).
- <sup>8</sup>N. Lee, D. M. Larsen, and B. Lax, J. Phys. Chem. Solids **34**, 1059 (1973).
- <sup>9</sup>M. C. Praddaude, Phys. Rev. **6A**, 1321 (1972).
- <sup>10</sup>Ed. R. Smith, R. J. W. Henry, G. L. Surlmelian, R. F. O'Connell, and A. K. Rajagopal, Phys. Rev. **6D**, 3700 (1972).
- <sup>11</sup>N. Lee, D. M. Larsen, and B. Lax, J. Phys. Chem. Solids **34**, 1817 (1973).
- <sup>12</sup>Y. Nisida and R. Horii, J. Phys. Soc. Jpn. **31**, 776 (1971).
- <sup>13</sup>N. Lee, D. M. Larsen, and B. Lax, J. Phys. Chem. Solids **35**, 401 (1974).
- <sup>14</sup>E. M. Gershenson, G. N. Gol'tsman, and M. L. Kagane, Zh. Eksp. Teor. Fiz. **72**, No. 4 (1976) [Sov. Phys. JETP **45**, No. 4 (1976)].
- <sup>15</sup>T. M. Lifshitz and F. Ya. Nad', Dokl. Akad. Nauk SSSR **162**, 801 (1965) [Sov. Phys. Dokl. **10**, 532 (1965)]; Sh. M. Kogan and B. I. Sedunov, Fiz. Tverd. Tela (Leningrad) **8**, 2382 (1966) [Sov. Phys. Solid State **8**, 1898 (1966)].
- <sup>16</sup>E. M. Gershenson and G. N. Gol'tsman, Fiz. Tekh. Pol-

- uprovodn. **6**, 580 (1972) [Sov. Phys. Semicond. **6**, 509 (1972)].
- <sup>17</sup>E. M. Gershenson, G. N. Gol'tsman, and N. G. Ptitsina, *Fiz. Tekh. Poluprovodn.* **7**, No. 6 (1973) [Sov. Phys. Semicond. **7**, No. 6 (1973)].
- <sup>18</sup>D. M. Larsen, *J. Phys. Chem. Solids* **29**, 271 (1968); S. Narita and M. Miyao, *Solid State Commun.* **9**, 2161 (1971).
- <sup>19</sup>H. R. Fetterman, D. M. Larsen, G. E. Stillman, P. E. Tannenwald, and J. Waldman, *Phys. Rev. Lett.* **26**, 975 (1971).
- <sup>20</sup>G. E. Stillman, D. M. Larsen, C. M. Wolfe, and R. C. Brandt, *Solid State Commun.* **9**, 2245 (1971).
- <sup>21</sup>R. A. Stradling, L. Eaves, R. A. Houlst, N. Miura, P. E. Simmonds, and C. C. Bradley, *Gallium Arsenid and Related Compounds*, Boulder, Colorado, 1972, ed. London, England, *Inst. Phys.*, 1973, pp. 65-74.
- <sup>22</sup>V. K. Baghenov, *Phys. Status Solidi B* **59**, K93 (1973); F. Bassani, G. Iadonisi, and B. Preziosi, *Phys. Rev.* **186**, 735 (1969).
- <sup>23</sup>J. Golka, *J. Phys. C* **22**, L407 (1974).
- <sup>24</sup>R. A. Faulkner, *Phys. Rev.* **184**, 713 (1969).
- <sup>25</sup>E. M. Gershenson, L. A. Orlov, and N. G. Ptitsina, *Pis'ma Zh. Eksp. Teor. Fiz.* **22**, 207 (1975) [JETP Lett. **22**, 95 (1975)].
- <sup>26</sup>Y. Nisida and K. Horii, *J. Phys. Soc. Jpn.* **26**, 388 (1969).
- <sup>27</sup>R. R. Haering, *Can. J. Phys.* **36**, 1161 (1958).
- <sup>28</sup>B. Pajot, F. Merlet, G. Taravella, and Ph. Arcas, *Can. J. Phys.* **50**, 1106 (1972).
- <sup>29</sup>L. D. Landau and E. M. Lifshitz, *Kvantovaya mekhanika (Quantum Mechanics)*, Fizmatgiz, 1963, p. 167 [Addison-Wesley 1965].
- <sup>30</sup>S. Zwerdling, K. J. Button, and B. Lax, *Phys. Rev.* **118**, 975 (1960).
- <sup>31</sup>B. Pajot, F. Merlet, and G. Taravella, *Can. J. Phys.* **50**, 2186 (1972).

Translated by J. G. Adashko

## Electron spin-lattice relaxation in a paramagnet at high pressures

G. N. Neïlo, A. D. Prokhorov, and G. A. Tsintsadze

*Donetsk Physico-technical Institute, Ukrainian Academy of Sciences*

(Submitted July 21, 1976)

*Zh. Eksp. Teor. Fiz.* **72**, 1081-1086 (March 1977)

Experimental results are presented on the variation of the electron spin-lattice relaxation time of a paramagnet during hydrostatic compression of the crystal. A significant effect of deformation on the relaxation process is discovered. It is shown that the relaxation transitions of two different magnetic ions can be bypassed by applying hydrostatic compression changing thereby the spin energy level system.

PACS numbers: 62.50.+p, 76.30.-v

### 1. INTRODUCTION

Studies of the EPR spectra of paramagnetic crystals subjected to an isotropic deformation at both high<sup>[1]</sup> and low<sup>[2,3]</sup> temperatures showed that external hydrostatic pressure gives rise to a fundamental change of the static properties of the crystal field, in particular, to a change of the symmetry type. The dynamics of the interaction of spin systems with a lattice is determined by the mechanism of the relaxation processes. The latter are characterized quantitatively by the electron spin-lattice relaxation time in paramagnetic crystals. This raises naturally another question concerning the effect of isotropic deformation on the dynamic parameters of the spin system: do the direct and Raman processes change (and to what extent) when the crystal is strongly deformed and the vibrational modes are correspondingly modified?

A paramagnetic cobalt ion (Co<sup>2+</sup>) implanted as a regular impurity in the trigonal lattice of diamagnetic zinc fluosilicate was selected for the experiments. The choice of the Co<sup>2+</sup> ion was dictated by the following considerations: first, the low level at which EPR is observed has a minimal twofold spin degeneracy, and, second, the electron relaxation of the Co<sup>2+</sup> ion at low

temperatures and normal pressure is described by both direct and Raman processes.<sup>[4]</sup>

### 2. MEASUREMENT TECHNIQUE

Since the data obtained here are, to the authors' knowledge, the results of the first experimental investigation of the electron spin-lattice relaxation at high pressures, a brief description of the distinguishing features of the measurement procedure is given below.

Optically homogeneous single crystals of zinc fluosilicate ZnSiF<sub>6</sub> · 6H<sub>2</sub>O grown from the solution by the temperature reduction method (in the temperature range 45-28 °C) were used to investigate the effect of high pressures on the electron spin-lattice relaxation of Co<sup>2+</sup> ions. The spin-relaxation measurements were carried out with an EPR pulsed relaxometer in the 3 cm band at pressures up to 13 kbar. The EPR signal was saturated with an additional klystron connected in the microwave circuit and tuned to the signal-generator frequency. Complete saturation of the EPR lines was attained at all pressures.

Since measurements of the spin-lattice relaxation time have their own distinctive features, that is: a) the